

THE SHAPES OF ATOMIC LINES FROM THE SURFACES OF WEAKLY MAGNETIC ROTATING NEUTRON STARS AND THEIR IMPLICATIONS

SUDIP BHATTACHARYYA,¹ M. COLEMAN MILLER,^{1,2} AND FREDERICK K. LAMB^{3,4}

Received 2004 December 6; accepted 2006 March 3

ABSTRACT

Motivated by the report by Cottam et al. of iron resonance scattering lines in the spectra of thermonuclear bursts from EXO 0748–676, we have investigated the information about neutron star structure and the geometry of the emission region that can be obtained by analyzing the profiles of atomic lines formed at the surface of the star. We have calculated the detailed profiles of such lines, taking into account the star’s spin and the full effects of special and general relativity, including light bending and frame dragging. We discuss the line shapes produced by rotational Doppler broadening and magnetic splitting of atomic lines for the spin rates and magnetic fields expected in neutron stars in low-mass X-ray binary systems. We show that narrow lines are possible even for rapidly spinning stars if the emission region or the line of sight are close to the spin axis. For most neutron stars in low-mass systems, magnetic splitting is too small to obscure the effects of special and general relativity. We show that the ratio of the star’s mass to its equatorial radius can be determined to within 5% using atomic line profiles, even if the lines are broad and skewed. This is the precision required to constrain strongly the equation of state of neutron star matter. We show further that if the radius and latitude of emission are known to $\sim 5\%$ – 10% accuracy, then frame dragging has a potentially detectable effect on the profiles of atomic lines formed at the stellar surface.

Subject headings: equation of state — line: profiles — relativity — stars: neutron — stars: rotation — X-rays: stars

1. INTRODUCTION

The discovery (Cottam et al. 2002) of line features in the average spectrum of 28 type I X-ray bursts from the neutron star in the low-mass X-ray binary (LMXB) EXO 0748–676 is a significant advance that provides new information on the structure of neutron stars and the properties of dense matter. The lines were detected using *XMM-Newton* and have been identified as resonance-scattering lines of Fe xxv $H\alpha$, Fe xxv 2–3, and possibly O VIII $Ly\alpha$. The gravitational redshifts inferred from the observed energies of all three lines are ~ 0.35 (Cottam et al. 2002), consistent with their formation at the surface of the star.

The profiles of atomic lines formed at the surface of a neutron star are affected not only by the gravitational redshift there, but also by the star’s radius, spin, angular momentum, and magnetic field. Such lines carry more information about the properties of the star, the equation of state (EOS) of cold, high-density matter, and the binary system than any other features of the star’s spectrum.

The X-ray burst oscillations of EXO 0748–676 show that the spin frequency of the neutron star in this system is 45 Hz (Villarreal & Strohmayer 2004), implying a line-of-sight rotational speed at the stellar surface $\lesssim 0.015c$ and a rotational Doppler width at most 10 times the Fe line width produced by Stark broadening (see Bildsten et al. 2003), even for the high system inclination $i \sim 75^\circ$ – 82° indicated by the dips and eclipses observed in this system (Parmar et al. 1986).

Spin rates as low as 45 Hz are expected only if the accretion phase has lasted less than the time required to spin up the star, or

the accretion rate is low enough or the star’s magnetic field strong enough that the star has reached spin equilibrium (Lamb & Yu 2005). Magnetic splitting by fields $\gtrsim 2 \times 10^9$ G would change the profiles of the Fe lines significantly, and fields an order of magnitude stronger would shift the energy E_0 of the line center (Loeb 2003). Consequently, the strength of the magnetic field in EXO 0748–676 and in other burst sources is an important issue.

Some 18 neutron stars in LMXBs have spin rates ranging from 200 to 600 Hz (see Lamb & Yu 2005), much higher than the spin rate of the neutron star in EXO 0748–676. Spin rates this high imply surface speeds near the rotational equator of 0.05 – $0.20c$. Atomic lines formed at the surfaces of such rapidly spinning stars may be broadened substantially by rotational Doppler broadening (Özel & Psaltis 2003). The magnitude of this broadening is an important issue in determining whether general relativistic effects can be detected.

Here we summarize the most important results of a detailed theoretical study of the effects of general relativity on the shapes of atomic spectral lines formed at the surfaces of spinning neutron stars. Some of these effects were illustrated by Özel & Psaltis (2003). We also discuss the evidence concerning the strengths of the magnetic fields of neutron stars in LMXBs and the implications for magnetic splitting of lines formed near their surfaces and for measurement of general relativistic effects.

We find that even lines formed at the surfaces of stars with spin rates as large as hundreds of Hertz observed at inclinations to the spin axis as high as $\sim 75^\circ$ can have relative widths $\delta E_0/E_0$ as small as 10^{-2} if they are formed predominantly within $\sim 10^\circ$ – 20° of the spin axis. We show that using the geometric mean of the energies of the line wings greatly reduces the systematic error in determinations of the star’s mass-to-radius ratio. We also show that the ratios of the depths of the red and blue flux minima of a resonance-scattering line provide a unique signature of frame dragging. In most neutron stars in low-mass systems, magnetic splitting of lines is too small to obscure the effects of special and general relativity

¹ Department of Astronomy, University of Maryland, College Park, MD 20742-2421.

² Also Maryland Astronomy Center for Theory and Computation.

³ Center for Theoretical Astrophysics, Loomis Laboratory of Physics, 1110 West Green Street, University of Illinois, Urbana, IL 61801-3080.

⁴ Also Departments of Physics and Astronomy, University of Illinois at Urbana-Champaign.

on their profiles. Finally, we discuss the prospects for detecting these relativistic effects. In the rest of this paper we use geometric units in which $c = G = 1$, unless otherwise stated.

2. PHYSICAL EFFECTS AND CALCULATIONAL METHOD

At a given instant, the X-ray-emitting portion of the neutron star surface could be a hot spot (produced, e.g., by magnetically channeled accretion, confined thermonuclear burning, or localized cooling gas), a belt (produced, e.g., by disk accretion near the rotational equator or rotationally confined thermonuclear burning), or a combination. Emission from a localized region that is not at the rotation pole is effectively smeared into an axisymmetric belt when averaged over many spin periods. This is to be expected for the spin frequencies $\gtrsim 10$ Hz of neutron stars in LMXBs and the integration times of seconds typical of current high-resolution spectroscopic measurements. We therefore treat the emission as coming from an axisymmetric belt and assume for simplicity that the belt is uniformly bright.

The profile of a spectral line formed at the stellar surface carries the imprint of several physical effects. Here we consider (1) magnetic (Zeeman or Paschen-Back) splitting by the star's magnetic field, (2) longitudinal and transverse Doppler shifts, (3) special relativistic beaming, (4) gravitational redshifts, (5) light bending, and (6) frame dragging. We treat the star as spherical, neglecting the effects of the spin-induced stellar oblateness and the deviation of the exterior spacetime from Kerr, which are small compared to the uncertainties.⁵

Effects (1)–(6) influence the line shape in different ways. Magnetic splitting, Doppler shifts, and the variation in the emitting area for a given observed energy cause an otherwise narrow scattering line to become broader and can cause it to have two minima. The gravitational redshift and transverse Doppler effect both shift the line toward lower energies. Special relativistic beaming deepens the blue minimum but suppresses (or eliminates) the red minimum, for emission from a belt around the star. Light bending deepens both minima, but deepens the red minimum more and can sometimes make visible a red minimum that was suppressed by special relativistic beaming. Finally, frame dragging broadens the line and shifts it slightly toward higher energies.

To compute detailed line shapes, we first assumed (1) an EOS, (2) a gravitational mass M , and (3) a stellar spin rate ν_s . We chose as a representative modern⁶ EOS the A18 + δv + UIX model of Akmal et al. (1998), which combines the Argonne v_{18} (A18) model of the two-nucleon interaction (Wiringa et al. 1995), the Urbana IX (UIX) model of the three-nucleon interaction (Pudliner et al. 1995), and relativistic boost corrections to the A18 interaction. Using this EOS, we determined the star's radius R and dimensionless angular momentum $j \equiv J/M^2$ by computing numerically and self-consistently the structure and interior spacetime of the star, following Cook et al. (1994; see Bhattacharyya et al. 2000 for a detailed description of the method we used).

We usually consider an emitting belt in the northern hemisphere specified by (4) the colatitude i_{belt}^p of its northernmost (polar) edge and (5) the colatitude $i_{\text{belt}}^{\text{eq}}$ of its southernmost (equatorial)

⁵ For a stellar model with a gravitational mass $\geq 1.4 M_\odot$ and a spin rate of 400 Hz as measured at infinity, constructed using the A18 + δv + UIX EOS (Akmal et al. 1998), the ratio of the polar radius to the equatorial radius is greater than 0.965; all other effects of the star's oblateness are at most a few percent. The Kerr spacetime is an accurate approximation to the exterior spacetime of a spinning neutron star only to first order in the spin; higher accuracy requires numerical computation of the spacetime (see Miller et al. 1998a).

⁶ Models that, like A18 + δv + UIX, fit the Nijmegen database (Stoks et al. 1993) with $\chi^2/N_{\text{data}} \sim 1$ are called “modern.”

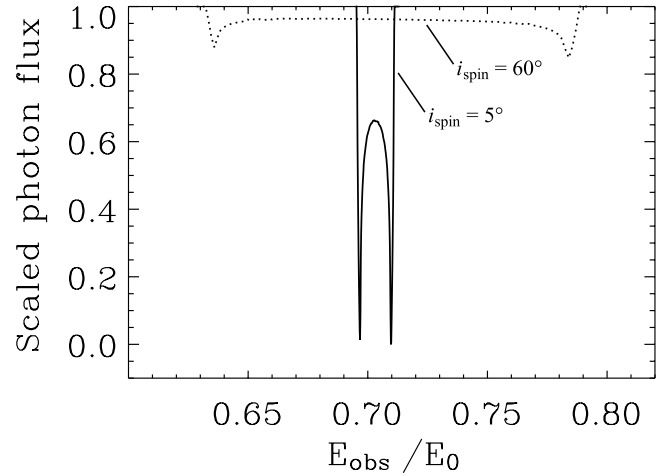


FIG. 1.—Profiles of a narrow line formed at the stellar surface as seen by observers at $i_{\text{spin}} = 5^\circ$ (solid profile) and $i_{\text{spin}} = 60^\circ$ (dotted profile), showing that such lines typically have two narrow flux minima. E_{obs}/E_0 is the energy of the observed radiation in units of the rest energy E_0 of the line center. Both profiles are for EOS model A18 + δv + UIX, $\nu_s = 400$ Hz, $R/M = 4.0$, $i_{\text{belt}} = 90^\circ$, $\Delta i_{\text{belt}} = 5^\circ$, and isotropic emission in the frame corotating with the stellar surface. The $i_{\text{spin}} = 5^\circ$ profile is scaled in units of its deepest flux minimum; the $i_{\text{spin}} = 60^\circ$ profile is scaled to have the same equivalent width.

edge. Alternatively, we specify the location and width of the belt by the colatitude i_{belt} of its center and its angular half-width Δi_{belt} . The emission from each point in the belt is specified in the corotating frame by (6) an intensity distribution of the form $I_\nu \propto \cos^n(\psi)$, where ψ is the angle measured from the local normal to the stellar surface and the parameter n specifies the degree of beaming. Except when we consider magnetic splitting, we assumed a boxcar intrinsic line shape with (7) a half width $\delta E_0 = 10^{-3} E_0$, where E_0 is the rest energy of the line center; this is comparable to the width expected from Stark broadening (Bildsten et al. 2003). The final parameter is (8) the inclination i_{spin} of the observer relative to stellar spin axis.

Given these eight parameters, we determine the image of the source seen by the observer by tracing the path of photons in the Kerr spacetime from the observer back to the source. We then compute the observed spectrum by integrating the energy-dependent specific intensity over the image (for a more detailed description of this procedure, see Bhattacharyya et al. 2001). Our method reproduces (for $j = 0.0$) the results of Özel & Psaltis for their parameter choices. The calculations reported here ignore instrumental broadening, to show what may be possible in the future.

3. RESULTS

The combined effects of magnetic splitting, Doppler shifts, special relativistic beaming, gravitational redshift, light bending, and frame dragging typically make lines broader, shallower, and skewed, and can create two flux minima (see Fig. 1, in which the profiles are scaled to have the same equivalent width). These effects do not weaken lines, contrary to what has sometimes been implied in the literature (see, e.g., Özel & Psaltis 2003): their equivalent widths remain unchanged. Note, however, that a broader and shallower line might be more difficult to detect.

Whether magnetic splitting is an important broadening mechanism depends on the strength of the star's surface magnetic field. Magnetic fields in the line-forming region with strengths $\gtrsim 10^{10}$ G would broaden and shift X-ray lines enough to make identification of the transitions and determination of the redshift and other stellar properties difficult (Loeb 2003). However, the

spin rates and other observed properties of neutron stars in LMXBs and the spin-down rates of recycled radio pulsars indicate that most neutron stars in LMXBs have magnetic fields $\sim 10^7$ – 10^9 G (Miller et al. 1998b; Lamb & Yu 2005), too weak to broaden Fe lines by more than ~ 20 eV.

The spin rate of the neutron star in EXO 0748–676 could be 45 Hz either because it has not accreted enough matter to reach a higher frequency or because its field is strong enough to maintain spin equilibrium at 45 Hz. Accretion will double the spin rate ν_s of a star far from spin equilibrium in $\sim 6 \times 10^6 (\dot{M}/0.03\dot{M}_E)^{-0.87} (\nu_s/45 \text{ Hz})$ yr, where \dot{M} is the accretion rate and $\dot{M}_E \approx 1.5 \times 10^{18} \text{ g s}^{-1}$ is the Eddington accretion rate onto a star with a 10 km radius (see Lamb & Yu 2005). The magnetic field required to maintain a 45 Hz spin rate is 2×10^9 G for accretion at the relatively high long-term average rate $\langle \dot{M} \rangle \sim 0.03\dot{M}_E$, or 1.5×10^8 G for $\langle \dot{M} \rangle \sim 10^{-4}\dot{M}_E$ (Lamb & Yu 2005). The splitting produced by 2×10^9 G would be ~ 20 eV, so it is unlikely that magnetic splitting dominates the line widths observed in EXO 0748–676, but it could contribute to them.

A line produced at the surface of a star that is spinning rapidly may nevertheless appear narrow if it is intrinsically narrow and (1) the colatitude $i_{\text{belt}}^{\text{eq}}$ of the region where the line is formed is sufficiently small, (2) the observer’s inclination i_{spin} relative to the spin axis is sufficiently small, or both angles are relatively small. For example, the observed width of Fe lines formed at the surface of a $1.5 M_\odot$ star observed at $i_{\text{spin}} \approx 75^\circ$ is only ~ 20 eV if $\nu_s = 200$ Hz and $i_{\text{belt}}^{\text{eq}} \lesssim 24^\circ$, or if $\nu_s = 600$ Hz and $i_{\text{belt}}^{\text{eq}} \lesssim 7^\circ$. Thus, narrow lines are possible even if $\nu_s = 600$ Hz, if they are preferentially formed near the rotation axis, as in a hotter region close to a nearly aligned magnetic pole (in some evolutionary scenarios, alignment of the magnetic axis with the spin axis is expected).

Scattering lines with two flux minima are possible for emission from any part of a spherical surface only if the emission is beamed in the rest frame of the surface or there is general relativistic light deflection; the depths of the resulting minima depend on the location and width of the emitting belt and i_{spin} .

Özel & Psaltis (2003) showed that if the redshift z_{surf} at the surface of the star is estimated using the energy of the deepest minimum in the full line profile, the distortion of the line profile by special and general relativistic effects can introduce errors of tens of percent for stars with spin rates of hundreds of Hz. Our study confirms this result (see Fig. 2).

We have found a way to reduce greatly the effects of the distortion of the line profile on measurements of z_{surf} . Using the quantity $(E_0/E_{\text{gm}}) - 1$, where $E_{\text{gm}} \equiv (E_1 E_2)^{1/2}$ is the geometric mean of the low-energy and high-energy edges of the observed line, yields very accurate estimates of z_{surf} , even if the line is broad and skewed. We explored this approach because, for surfaces rotating at speed β toward and away from the observer, the lower and higher energy edges of the line are Doppler shifted to $E_1 = E_0\gamma(1 - \beta)$ and $E_2 = E_0\gamma(1 + \beta)$, where $\gamma \equiv (1 - \beta^2)^{-1/2}$ is the Lorentz factor. E_{gm} is therefore exactly equal to E_0 in this geometry, when light bending is neglected. Our calculations show that using the geometric mean of the energies of the two flux minima also yields a very accurate estimate of z_{surf} .

Figure 2 compares the value of R/M estimated using E_{gm} with the true equatorial value of R/M and the values estimated using (1) the geometric means of the energies of the lower and higher energy flux minima and edges of the line, (2) the arithmetic means of the energies of lower and higher energy flux minima and the energies of the lower- and higher-energy edges of the line, and (3) the energy of the deepest flux minimum in the line profile, assuming that the line is formed in the region between colatitude 60° and the rotational equator 90° . The error in R/M is greater

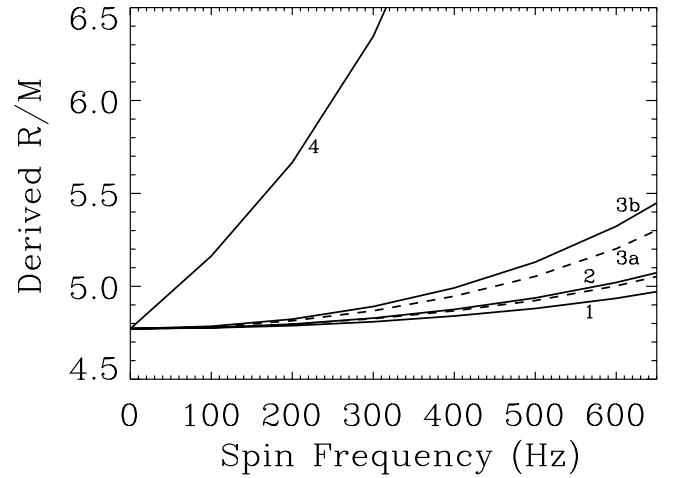


FIG. 2.— Accuracy of R/M estimates using different methods. Curve 1: true equatorial value of R/M as a function of the stellar spin frequency. Curve 2: R/M estimates based on the geometric mean of the energies of the two narrow photon flux minima in the line profile (dashed curve) and the lower and higher energy edges of the line (solid curve). See text for details. For the parameters assumed here, these two methods give nearly identical estimates. When these methods are used, the error in R/M is typically less than 2%, even for spin frequencies as high as 600 Hz. Curves 3a and 3b: estimates based, respectively, on the arithmetic mean of the energies of the flux minima and the energies of the lower and higher energy edges of the line. Curve 4: estimates based on the energy of the deepest flux minimum in the line profile. All curves are for EOS model A18 + δv + UIX, $M = 1.6 M_\odot$, $i_{\text{spin}} = 90^\circ$, $i_{\text{belt}}^p = 60^\circ$, $i_{\text{belt}}^{\text{eq}} = 90^\circ$, and isotropic emission in the frame corotating with the stellar surface.

when R/M is estimated from the energy of the deepest flux minimum in a line profile formed over a range of latitudes than in a line formed uniformly over the whole stellar surface (see Özel & Psaltis 2003), but the former geometry is probably more realistic.

The value of R/M estimated using E_{gm} differs from the ratio of the star’s equatorial radius R_{eq} to M by less than 1.7% for $\nu_s < 600$ Hz (see Fig. 2). Even if the line is formed over the whole surface of the star, the geometric mean gives a much better estimate of R/M than does the energy of the deepest flux minimum. Using the arithmetic mean of the energies of the two flux minima or the energies of the lower and higher energy edges of the line gives estimates of R/M that differ from R_{eq}/M by up to 7.3% and 57.0%, respectively.

The estimated value of R/M deviates most from the true value when the star spins rapidly, R/M is small (for a fixed EOS model and stellar spin), or the band is centered at the spin equator. We find that the accuracy is independent of the beaming parameter n . In all of the combinations of parameters we have tried, the accuracy in R/M using our method is better than 2% when $\nu_s = 600$ Hz. In Figures 3 and 4 we show the dependence of the estimates on the true values of R/M and belt locations and widths.

Importantly, we have found a possible signature of frame dragging in the line profile, which could be used to detect frame dragging if $R \sin i_{\text{spin}}$ is known to better than $\sim 5\%$ – 10% . As pointed out by the anonymous referee, the effect of frame dragging for a given angular velocity is to decrease the linear speed of the surface relative to the locally nonrotating frame (also see Poutanen & Gierliński 2003). The angular velocity of frame dragging at the surface is typically $\sim 10\%$ – 20% of the stellar spin rate. As seen in Figure 5, this affects the ratio of the depth of the low-energy (red) flux minimum to the depth of the high-energy (blue) flux minimum, which increases steeply with increasing j , but either decreases or increases only slowly with variations of most other parameters. This effect is also produced by changing the linear surface speed at a fixed spin frequency, i.e., by changing $R \sin i_{\text{spin}}$.

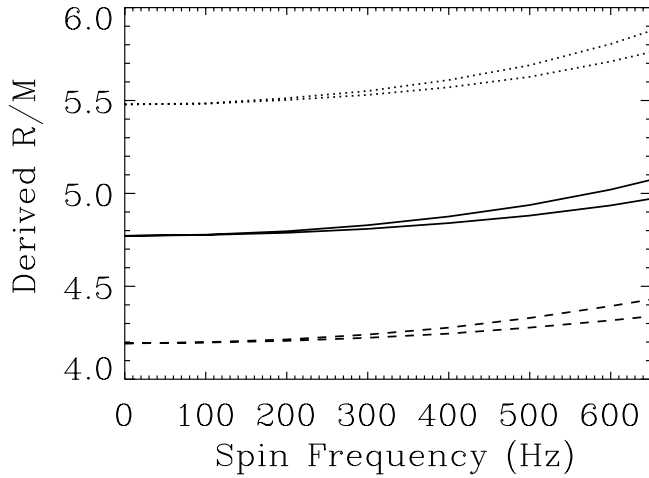


FIG. 3.—Accuracy of R/M estimates for different stellar mass (M) values. In each of the three sets of curves, the lower curve gives the true equatorial value of R/M as a function of the stellar spin frequency. The corresponding upper curve gives the estimate of R/M based on the geometric mean of the energies of the lower and higher energy edges of the line (see text for details). The dotted curves are for $M = 1.4 M_{\odot}$, the solid curves for $M = 1.6 M_{\odot}$, and the dashed curves for $M = 1.8 M_{\odot}$. The values of the other parameters are same as in Fig. 2. The percentage error in R/M estimate very slowly increases with the increase of M (or the decrease of R/M when the other independent parameters remain same).

Because $R \sin i_{\text{spin}}$ also affects the width of the full line profile, a precise ($\sim 5\%$ – 10%) measurement of line width (and hence $R \sin i_{\text{spin}}$) could allow detection of frame-dragging effects.

If such precision is possible (e.g., with a future high throughput and high resolution mission such as Constellation-X), then the most robust way to detect this effect is to measure the overall asymmetry of the line, using as a reference the local flux maximum ϕ_m at E_m , between the two flux minima at E_1 and E_2 . The photon flux is equal to ϕ_m at two other energies, $E_{m1} < E_m$ and $E_{m2} > E_m$, but less than ϕ_m at all energies between E_{m1} and E_{m2} . There is therefore a “red flux deficit” from E_{m1} to E_m relative to $\phi_m(E_m - E_{m1})$ and a “blue flux deficit” from E_m to E_{m2} relative

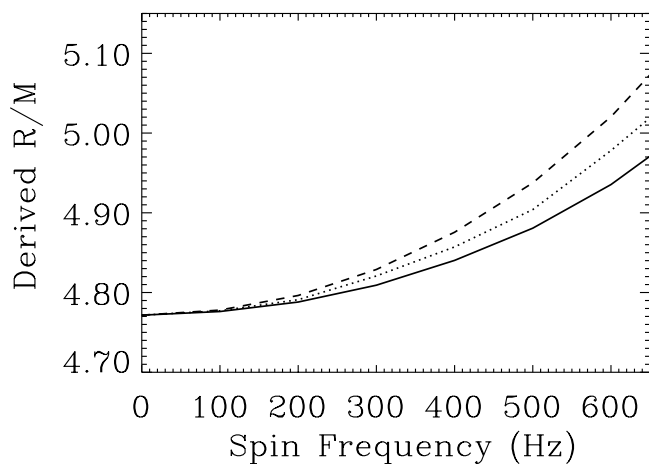


FIG. 4.—Accuracy of R/M estimates for different belt locations and belt widths. The solid curve gives the true equatorial value of R/M for EOS model A18 + δv + UIX and $M = 1.6 M_{\odot}$. The geometric means of the energies of the lower and higher energy edges of the line are the same for the following three belt locations and widths: (1) belt covering the whole stellar surface, (2) $i_{\text{belt}}^p = 60^\circ$ and $i_{\text{belt}}^{\text{eq}} = 90^\circ$, and (3) $i_{\text{belt}} = 90^\circ$, $\Delta i_{\text{belt}} = 5^\circ$. The dashed curve gives the estimate of R/M based on these mean energies. The dotted curve gives the estimate of R/M for $i_{\text{belt}} = 30^\circ$, $\Delta i_{\text{belt}} = 5^\circ$. For all the curves $i_{\text{spin}} = 90^\circ$ and the emission is isotropic in the frame corotating with the stellar surface.

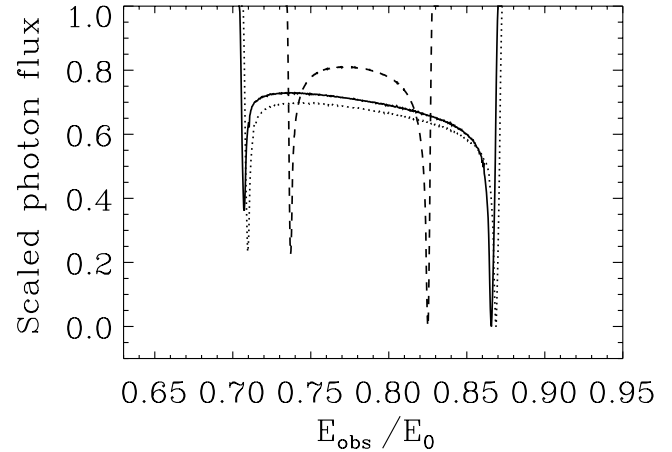


FIG. 5.—Profiles of narrow lines formed at the stellar surface as they would appear to an observer at $i_{\text{spin}} = 60^\circ$ if $j = 0.0$ (solid profile) and if $j = 0.188$ (dotted profile), showing that measurements of the depths of the flux minima could be used to detect the general relativistic dragging of inertial frames. E_{obs}/E_0 is the energy of the observed radiation in units of the rest energy of the line. For each of the profiles the flux has been scaled to have a minimum value of 0 and a maximum value of 1. Both profiles assume EOS model A18 + δv + UIX, $M = 1.5 M_{\odot}$, $i_{\text{belt}} = 90^\circ$, $\Delta i_{\text{belt}} = 5^\circ$, and isotropic emission in the frame corotating with the stellar surface. For this EOS and mass, $j = 0.188$ for $\nu_s = 400$ Hz. A third profile (dashed; for $i_{\text{spin}} = 30^\circ$ and $j = 0.0$ all other parameter values are same, scaled in the same way as the other two profiles) is displayed to show that, although the frame dragging and a lower value of i_{spin} have the similar effects on the depths of the flux minima, these two causes can be distinguished by the width of the line profile.

to $\phi_m(E_{m2} - E_m)$. Like equivalent widths, these flux deficits depend only weakly on the detector’s resolution, which will make this easier to detect in practice. If the required precision can be attained, we note that a quantitative measure of j will provide a constraint on the properties of high-density matter that is independent of, e.g., measurements of R/M . We do note that in practice the detection of this effect will be made more complicated if other processes introduce red-blue asymmetry, such as the fine-structure splitting discussed by Chang et al. (2005).

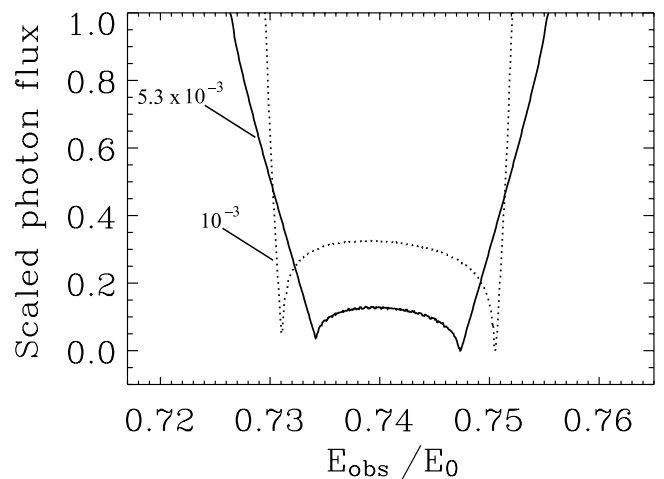


FIG. 6.—Effect on line profiles of additional broadening, such as that produced by unresolved Zeeman splitting. Shown are the observed profiles of lines with intrinsic half widths of $10^{-3} E_0$ (dotted curve; the same as in the other line profile calculations reported here) and $5.3 \times 10^{-3} E_0$ (solid curve; half the half width produced by rotational Doppler broadening, comparable to the splitting produced by a 10^9 G magnetic field). For each of the profiles the flux has been scaled in units of its deepest minimum. Both profiles are for $R/M = 4.43$, $R = 11.5$ km, $\nu_s = 45$ Hz, $i_{\text{belt}} = 90^\circ$, $\Delta i_{\text{belt}} = 5^\circ$, isotropic emission in the frame corotating with the stellar surface, and $i_{\text{spin}} = 78^\circ$.

Figure 5 illustrates the effect of j on the flux deficit ratio, when the other parameters in the problem (including ν_s) remain fixed. Both profiles are normalized by their maximum depths. In this example, the flux deficit ratio is $\sim 36\%$ greater for $j = 0.188$ ($\nu_{\text{spin}} = 400$ Hz) than for $j = 0$.

Figure 6 demonstrates that the double flux minima remain visible even if other broadening mechanisms, such as Zeeman splitting, make the intrinsic line width substantially greater than it would otherwise be. Shown are the predicted profiles of lines with intrinsic half widths of $10^{-3}E_0$ (the same as in the other line profile calculations reported here) and $5.3 \times 10^{-3}E_0$ (half the half width produced by rotational Doppler broadening). The latter half width is similar to the magnetic splitting produced by a 10^9 G magnetic field, comparable to the field required to maintain a neutron star with a long-term average accretion rate $\langle \dot{M} \rangle \sim 0.03 \dot{M}_E$ in spin equilibrium at the 45 Hz spin rate of EXO 0748–676.

4. DISCUSSION AND CONCLUSIONS

The discovery of line features in the spectrum of EXO 0748–676 by Cottam et al. (2002) motivated us to explore the information that can be obtained from analysis of the profiles of atomic lines formed at the surfaces of neutron stars. We confirm the finding of Villarreal & Strohmayer (2004), that the widths of these features are consistent with formation at the surface of a star with a spin rate of 45 Hz. We have also shown that stars with spin rates up to ~ 600 Hz can produce lines this narrow if emission from close to the rotational axis dominates. Confirmation of these features by future observations, or detection of surface lines from other LMXBs, will help strengthen and clarify this picture.

We have demonstrated that the radius-to-mass ratio R/M can be inferred from spectral line profiles with very little (in general less than 2%) systematic error if the geometric mean of the energies of the two flux minima (instead of the energy of the deepest flux minimum) or two line edges is used. Observed line profiles can therefore be used to constrain EOS models to the 5% accu-

racy required to distinguish between different equations of state (Lattimer & Prakash 2001). Finally, we show that neutron star atomic spectral lines can be used to detect frame dragging. Such a detection would require observation of a line profile with two moderately well-resolved flux minima.

With the discovery of strong evidence for resonance-scattering lines formed at the surface of one neutron star, it can be hoped that current and future X-ray missions will be able to detect more such spectral lines. A strong and well-resolved broad line would provide a wealth of information about the neutron star. One candidate line is the Fe $K\alpha$ line, given the expected surface temperature and abundance of iron in accreting sources. Future X-ray spectroscopy missions will do even better. For example, Constellation-X will have a resolution and an effective area several times greater than those of *Chandra* and *XMM*. Detection and precise measurement of the properties of atomic lines formed at the surfaces of neutron stars would open a new avenue for studying dense matter, neutron stars, and LMXBs. Simultaneous observations of lines and burst oscillations by future, even more capable instruments could make possible phase-resolved line spectroscopy, using the light curve of the burst oscillation to determine the rotational phase of the star.

We thank Arun V. Thampan for providing the code used to compute the structure of rapidly spinning neutron stars and Geoff Ravenhall for providing tabulations of the $A18 + \delta v + \text{UIX}$ equation of state. We also appreciate the particularly useful comments about frame dragging provided by the anonymous referee. This work was supported in part by a National Science Foundation (NSF) grant AST 00-98436 at Maryland, by NSF grant AST 00-98399 and NASA grants NAG5-12030 and NAG5-8740 at Illinois, and by the funds of the Fortner Endowed Chair at the University of Illinois.

REFERENCES

- Akmal, A., Pandharipande, V. R., & Ravenhall, D. G. 1998, *Phys. Rev. C*, 58, 1804
- Bhattacharyya, S., Bhattacharya, D., & Thampan, A. V. 2001, *MNRAS*, 325, 989
- Bhattacharyya, S., Thampan, A. V., Misra, R., & Datta, B. 2000, *ApJ*, 542, 473
- Bildsten, L., Chang, P., & Paerels, F. 2003, *ApJ*, 591, L29
- Chang, P., Bildsten, L., & Wasserman, I. 2005, *ApJ*, 629, 998
- Cook, G. B., Shapiro, S. L., & Teukolsky, S. A. 1994, *ApJ*, 424, 823
- Cottam, J., Paerels, F., & Méndez, M. 2002, *Nature*, 420, 51
- Lamb, F. K., & Yu, W. 2005, in *ASP Conf. Ser. 328, Binary Radio Pulsars*, ed. F. A. Rasio & I. H. Stairs (San Francisco: ASP), 299
- Lattimer, J. M., & Prakash, M. 2001, *ApJ*, 550, 426
- Loeb, A. 2003, *Phys. Rev. Lett.*, 91, 1103
- Miller, M. C., Lamb, F. K., & Cook, G. B. 1998a, *ApJ*, 509, 793
- Miller, M. C., Lamb, F. K., & Psaltis, D. 1998b, *ApJ*, 508, 791
- Özel, F., & Psaltis, D. 2003, *ApJ*, 582, L31
- Parmar, A. N., White, N. E., Giommi, P., & Gottwald, M. 1986, *ApJ*, 308, 199
- Poutanen, J., & Gierliński, M. 2003, *MNRAS*, 343, 1301
- Pudliner, B. S., Pandharipande, V. R., Carlson, J., & Wiringa, R. B. 1995, *Phys. Rev. Lett.*, 74, 4396
- Stoks, V. G. J., Klomp, R. A. M., Rentmeester, M. C. M., & de Swart, J. J. 1993, *Phys. Rev. C*, 48, 792
- Villarreal, A. R., & Strohmayer, T. E. 2004, *ApJ*, 614, L121
- Wiringa, R. B., Stoks, V. G. J., & Schiavilla, R. 1995, *Phys. Rev. C*, 51, 38